

A comparison of two heavy rain events during the Terrain-influenced Monsoon Rainfall Experiment (TiMREX) 2008

2008 地形影響季風降雨實驗期間兩劇烈降水事件的比較

Chuan-Chi Tu 涂絹琪, Yi-Leng Chen 陳宇能

Department of Meteorology, University of Hawaii at Manoa, Honolulu, Hawaii

Ching-Sen Chen 陳景森, Pay-Liam Lin 林沛練

Institute of Atmospheric Physics, National Central University, Chung-Li, Taiwan
and

Po-Hsiung Lin 林博雄

Department of Atmospheric Sciences, National Taiwan University, Taipei, Taiwan

Abstract

Two heavy rainfall events during Taiwan's Mei-Yu season with daily rainfall maximums along the windward mountain range (31 May 2008) ($> 110 \text{ mm day}^{-1}$) and the coast (16 June 2008) ($> 200 \text{ mm day}^{-1}$) were studied and compared. For both cases, the existence of a moisture tongue from the tropics provided moisture source for pronounced latent heat release associated with the Mei-Yu system, which led to PV generation and intensification of a Mei-Yu mesocyclone.

During the daytime of 31 May, after the shallow surface front ($< 1 \text{ km}$) originated from north of Taiwan passed central Taiwan, the 850-hPa Mei-Yu mesocyclone moved toward western Taiwan. The orographic lifting of the prevailing warm, moist west-southwesterly flow aloft with a large westerly wind component ahead of the mesocyclone combined with sea breeze-upslope flow at the surface, provided the localized lifting needed for the development of heavy precipitation over the southwestern windward slopes.

On 16 June, pronounced orographic blocking of the warm, moist south/southwesterly flow by the terrain under the presence of relatively cold air at low levels due to a combination of nocturnal and rain evaporative cooling was important for the intensification of convective systems as they drifted inland and interacted with the land breezes. Furthermore, with a mountain-parallel flow aloft, orographic lifting aloft was absent. As a result, convective cells diminished as they moved in land. Over northern Taiwan, sea breeze/offshore flow developed over a leeside convergence zone in the afternoon hours resulting in heavy thunder showers ($> 110 \text{ mm day}^{-1}$).

Keywords: heavy rainfall, moisture tongue, latent heat release, PV, Mei-Yu mesocyclone, orographic, land/sea breezes

關鍵字: 劇烈降水, 溼舌, 潛熱釋放, 位渦, 梅雨中尺度氣旋, 地形的, 海陸風

1. Introduction

The precipitation and airflow over Taiwan during the early summer monsoon rainfall season are significantly modulated by the diurnal heating cycle (Johnson and Bresch 1991; Yeh and Chen 1998; Kerns et al. 2010). Along the western and southwestern windward coasts, the hourly rainfall frequencies have a very weak early morning maximum under the southwesterly monsoon flow (Yeh and Chen 1998; Kerns et al. 2010). From the principal component analysis (PCA) of surface variables during the Taiwan Area Mesoscale Experiment 1987 (TAMEX) (Kuo and Chen 1990), Chen and Li (1995) show that under the southwest monsoon flow, island blocking (Li and Chen 1998) exhibits diurnal variations which are most significant before sunrise. Linear convective lines along the land-breeze front off the northwestern coast were also observed from radar data in the early morning during the TAMEX Intensive Observing Period (IOP) #13 (Li et al. 1997). Recent statistics of heavy rainfall events show that most of the heavy rainfall events over southwestern Taiwan originated from pre-existing convective showers or mesoscale convective systems (MCSs) that drifted inland and interacted with the terrain and local winds (C.-S. Chen et al., 2007; 2008). The weak early morning rainfall maximum along the western and southwestern windward coasts occurs only under the southwesterly monsoon flow during the warm season and is likely caused by the convergence between the offshore flow and the incoming, decelerating southwesterly flow when the land surface is the coldest (Kerns et al. 2010). Along the southwestern coast, the occurrence of rain rates $> 15 \text{ mm h}^{-1}$ also has a weak early morning (0600-0700 LT) maximum (C.-S. Chen et al. 2007). In some cases, the rainfall maximum along the southwestern coast may occur during the daytime because of orographic blocking as the deflected flow turns into a southerly flow parallel to the orientation of the CMR (C.-S. Chen et al. 2005).

In this study, we use high resolution data collected during TiMREX (2008) to compare the mechanisms of two contrasting heavy rainfall events along the windward mountain range ($> 1 \text{ km}$) (31 May during IOP#3) and over the southwestern coast of Taiwan (16 June during IOP#8)(Fig. 1) through the case study approach. First of all, we would like to study the large-scale settings for the development of these two heavy precipitation events, including the role played by moisture tongues (embedded within the southwesterly monsoon flow) in deepening the Mei-Yu trough and enhancing

mesocyclones over southeastern China, the northern South China Sea, and the Taiwan area.

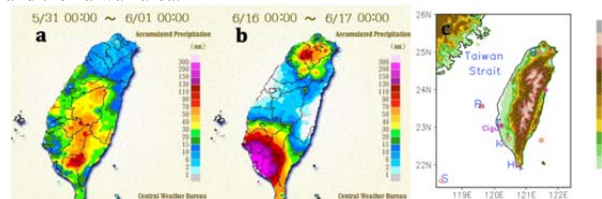


Fig. 1. Daily (0000-2400 Local Time) rainfall accumulation (mm) on (a) 31 May and (b) 16 June. (c) Terrain height for Taiwan (m). Banciao (121.43°E, 25°N), Penghu (119.63°E, 23.56°N), Tainan (Yongkang; Cigu Radar, 120.23°E, 23.04°N), Kaohisung (120.31°E, 22.57°N), Hengchun (120.74°E, 22.01°N), and South Ship (118.36°E, 21.46°N) stations are located at B, P, T, K, H and S, respectively. Red "o" marks rawinsonde site. Purple "+" marks Doppler radar site.

The main reasons that account for the differences in the timing and location of heavy rainfall between these two cases are examined in this study. For 16 June case (IOP#8), Xu et al. (2012) viewed the initiation and maintenance of the long-lived heavy-precipitation MCSs upstream of southwestern Taiwan through the "back-building/quasi-stationary" process. The convection developed continuously near the boundary of (1) the warm, moist unstable air mass associated with a LLJ over the upstream ocean and (2) a remnant cold pool generated by prior precipitation and orographic effects over southwestern Taiwan and the adjacent oceans. They also found that the coastal rainfall maxima were produced primarily by stratiform precipitation evolving from the upstream convection under relatively cold (near surface) and calm conditions over the island. Davis and Lee (2012) also suggested that the offshore warm moist LLJ lifted by a quasi-steady shallow frontal boundary caused by rain evaporative cooling over southwestern Taiwan is important for the initiation and intensification of convective cells as they drifted inland. In this study, the impinging angle of prevailing flow over southwestern Taiwan, and the land-sea thermal contrast between these two cases will be compared, with a focus on the physical processes leading to the heavy convective rainfall over the mountainous interior (IOP#3) and the stratiform rainfall along the coast (IOP#8). In particular, we wish to address the following questions: How do the terrain, diurnally driven local winds and rain evaporative cooling from pre-existing convection affect the

mesoscale convective systems embedded in the southwesterly monsoon flow as they drift inland? Why is the localized heavy rainfall concentrated over the southwestern coast of Taiwan with decreasing rainfall inland for the IOP#8 case? In addition, we also would like to study the mechanisms for the development of localized afternoon heavy rainfall associated with thunderstorm activity over northern Taiwan (Fig. 1b).

2. Data and Methodology

Radar reflectivities at Cigu (Fig. 1c) operational Doppler radar station are used to analyze the evolution of coastal MCSs over southwestern Taiwan during IOP#8. Daily rainfall accumulation maps were generated from 429 rainfall stations, which comprised conventional weather stations and Automatic Rainfall and Meteorological Telemetry System (ARMTS) (Kerns et al. 2010). The surface wind and temperature data from conventional surface weather stations are used to study the island-induced airflow (e.g. blocking of airflow and the diurnally driven flow) under disturbed Mei-Yu conditions. Time series of surface air temperature over southwestern Taiwan and the South Ship (Stations P, T, K, H and S in Figure 1c) will also be used to delineate low-level thermodynamic structure resulting from nocturnal and evaporative cooling during IOP#8. We use the temperature at the lowest level of shipboard soundings launched every 6 h as the surface air temperature at the South Ship. Note that during 14-16 June, the location of the South Ship is not stationary. Its path was shown in Davis and Lee (2012).

To address the challenge of tropical convection, World Climate Research Programme (WCRP) and World Weather Research Programme/The Observing System Research and Predictability Experiment (WWRP/THORPEX) conduct a framework of coordinated observing, modeling and forecasting of organized tropical convection, known as Year of Tropical Convection (YOTC) (Waliser et al. 2012). In this study, we will use the YOTC model analysis wind, pressure, moisture, and thermodynamic fields with $0.125^\circ \times 0.125^\circ$ resolution data (http://data-partial.ecmwf.int/data/d/yotc_rd) provided by the joint project of the WWRP/THORPEX and WCRP to study the airflow and thermodynamic fields in two heavy rainfall cases during TiMREX.

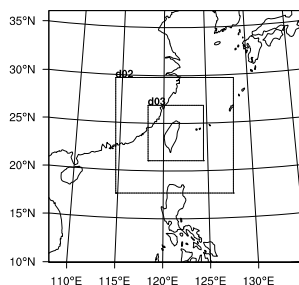


Fig. 2. The three domains for WRF model simulation with horizontal resolution of 27km, 9km, and 3km, respectively.

The WRF-ARW model (Skamarock et al. 2008) is used to simulate the events and assess the impact of latent heat (LH) release on the deepening and intensifying of the low-level Mei-Yu frontal mesocyclone (IOP#3) and an upper-level mesocyclone (IOP#8) within the prefrontal moisture tongue through modeling sensitivity test. PV and circulation associated with Mei-Yu mesocyclones simulated in the domain 2 (9 km resolution) (Fig. 2) will be compared between the control run (CTRL) and without LH release run (WOLH). The CTRL run is setup as described below. There are 38 sigma levels¹ from the surface to the 50-hPa level. The Rapid Radiative Transfer Model (RRTM) (Mlawer et al. 1997), Dudhia (1989) radiation schemes, Noah land-surface model (LSM) (Chen and Dudhia 2001) and Yonsei University (YSU) planetary boundary layer scheme (Hong et al. 2006) are used. The Ferrier microphysics scheme (Rogers et al. 2001; Ferrier et al. 2002) with diagnostic

¹ The full sigma levels are 1.000, 0.994, 0.983, 0.968, 0.950, 0.930, 0.908, 0.882, 0.853, 0.821, 0.788, 0.752, 0.715, 0.677, 0.637, 0.597, 0.557, 0.517, 0.477, 0.438, 0.401, 0.365, 0.332, 0.302, 0.274, 0.248, 0.224, 0.201, 0.179, 0.158, 0.138, 0.118, 0.098, 0.078, 0.058, 0.038, 0.018, 0.000

mixed-phase processes is employed. The Ferrier grid-scale cloud and precipitation scheme predicts variations of six species of water substances (cloud water, cloud ice/small ice crystals, rain, snow, graupel and sleet). The Betts-Miller-Janjic (BMJ) cumulus parameterization scheme (Janjic 1994, 2000), a column moist adjustment scheme relaxing towards a well-mixed profile (Skamarock et al. 2008), is chosen for simulation of deep convection within the Mei-Yu system that contributed to heavy rainfall. The cumulus parameterization is not applied in the 3 km resolution domain (domain 3). The National Centers for Environmental Prediction Final Analysis (NCEP FNL) data, with an one-degree horizontal resolution, provide the initial and boundary conditions for the model simulation. A 0.5° daily, real-time, global, sea surface temperature (RTG_SST) analysis developed at the National Centers for Environmental Prediction/Marine Modeling and Analysis Branch (NCEP/MMAB) are used to force the low boundary (Gemmill et al. 2007). Removing the latent heating effect of microphysics was accomplished by setting only the temperature tendency terms in the microphysics module equal to zero in the WOLH simulation. Additionally, BMJ cumulus scheme was turned off.

The low-level winds, land-sea thermal contrast, radar reflectivities simulated from 3 km resolution domain (domain 3) help to understand interactions between the regional monsoonal flow and local circulations in producing heavy rainfall during IOP#3 and IOP#8. The model is initialized at 0000 UTC 30 May and runs through 0600 UTC 31 May for IOP#3 case (30 h). It is initialized at 1200 UTC 15 June and runs through 0600 UTC 16 June for IOP#8 case (18 h).

3. Intensive Observation Period #3

a. Low-level Mei-Yu cyclonegenesis along the frontal boundary within the moisture tongue

From 1200 UTC 29 May to 0600 UTC 30 May 2008, as an upper-level trough originated in the leeside of the Yun-Gue Plateau over southern China and moved eastward over the moisture tongue over the southeastern China (Fig. 3), a Mei-Yu mesocyclone deepened (Fig. 4) within the moisture tongue (Fig. 3d). From the model sensitivity test, the mesocyclone intensified due to LH release associated with the Mei-Yu system over southeastern China was evident (Fig. 4). At 1200 UTC 30 May, LH release associated with Mei-Yu frontal rainband (Fig. 4b) deepened the Mei-Yu trough and generated significant PV at low-levels (Fig. 4a), which led to genesis of a Mei-Yu frontal mesocyclone over southeast coast of China with a strengthened cyclonic flow (Fig. 4b). Without LH release, relative weak cyclonic flow associated with Mei-Yu trough laid across Taiwan (Fig. 4d).

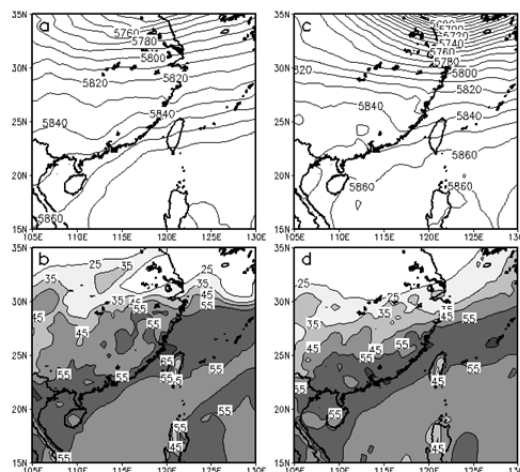


Fig. 3. YOTC (a) 500-hPa geopotential height (gpm) and (b) total precipitable water (mm) at 1200 UTC 29 May 2008. (c) 500-hPa geopotential height (gpm) and (d) total precipitable water (mm) at 0600 UTC 30 May.

b. Rainfall maximum along the windward slope of the southwestern Taiwan

On 31 May, the frontal mesocyclone moved southeastward over the Taiwan area (Fig. 5). At 0000 UTC (0800 LT) 31 May 2008,

at the 925-hPa level, the low-level westerly/southwesterly flow ahead of the mesoscale cyclone was deflected by the Central Mountain Range with southerly flow paralleling to the CMR over western Taiwan (Fig. 5a). The southwesterly flow and the deflected southerly flow converged with the postfrontal northeasterly flow (Fig. 5a) and land breezes (not shown) at the central western Taiwan coast resulted in the development of deep convection along the frontal boundary at the coast (Fig. 5a). At 0600 UTC (1400 LT), above the shallow postfrontal northeasterlies (~1 km) (Fig. 5c), the warm and moist westerlies (Fig. 5b) impinged on the CMR during the day. Thus, during the passage of the upper-level shortwave trough (not shown), deep convection could possibly develop over the windward mountain slopes and mountain interior of central Taiwan (Fig. 5b) behind the surface front (Fig. 5c). The development of this broad area convective system in the afternoon (Fig. 5b) was related to orographic lifting of the pre-existing convective cell along the frontal boundary that propagated inland (Figs. 5 and 6). In addition, the warm, moist southwesterly flow ahead of the frontal mesolow combined with sea breezes-upslope flow provided the low-level lifting on the windward slopes during the passage of the upper-level short-wave trough.

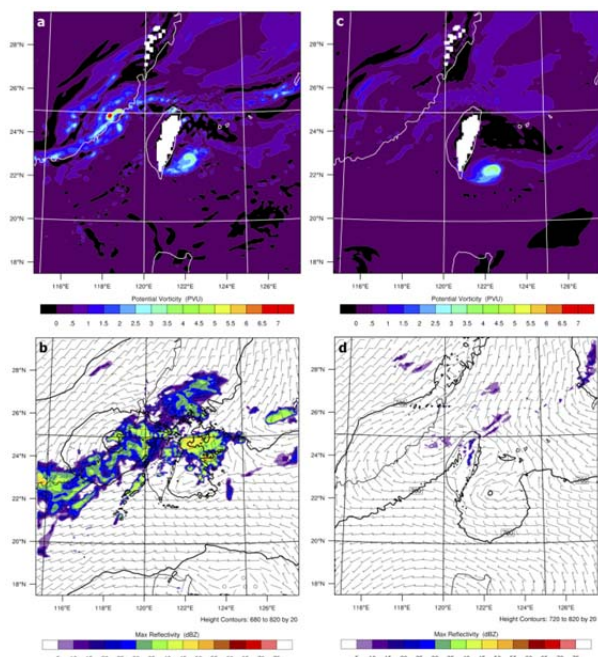


Fig. 4. WRF simulated 925-hPa (a) PV (PVU), (b) geopotential height (gpm, contoured), winds (1 barb= 10 m s^{-1}) and maximum reflectivity (dBZ, shaded) at 1200 UTC (2000 LT) 30 May in control (CTRL) run. (c) and (d): without latent heat release (WOLH) run (model is initialized at 0000 UTC 30 May) (Domain 2, 9km resolution).

4. Intensive Observation Period #8

a. Intensification of an upper-level mesocyclone over the prefrontal moisture tongue

At 1800 UTC 15 June (0200 LT 16 June), a broad upper-level low/trough laid over Taiwan and northern South China Sea (Fig. 7a) within the prefrontal moisture tongue (Fig. 7c). A 500-hPa vorticity maximum (Fig. 7b) was associated with the upper-level low over Taiwan (Fig. 7a). From the model sensitivity test, latent heat release associated with MCSs (Fig. 8) within the moisture tongue (Fig. 7c) is important for the intensification of the upper-level mesocyclone over the Taiwan and northern South China Sea (Fig. 8). Without LH release, weak upper-level mesocyclone laid over west of Taiwan (Fig. 8b). It is evident that the condensation heating associated with the convective clouds and anvils within MCSs led to PV generation at upper levels and intensification of the upper-level mesocyclone (Fig. 8).

b. Rainfall maximum along the coast of southwestern Taiwan

At 1800 UTC 15 June (0200 LT 16 June), a high equivalent potential temperature (Θ_e) axis at the 850-hPa level (Fig. 7c), corresponding to the moist tongue discussed earlier, was also evident. It is apparent that the moist tongue, rooted in the deep tropics, contributed to the convective instability over the South China Sea and Taiwan. In addition, the 500-hPa vorticity maximum associated with the mesolow over Taiwan was advected southwestward by the thermal wind (Figs. 7a and 7b) which was favorable for the development of convective activity off southwest coast of Taiwan (Fig. 9a).

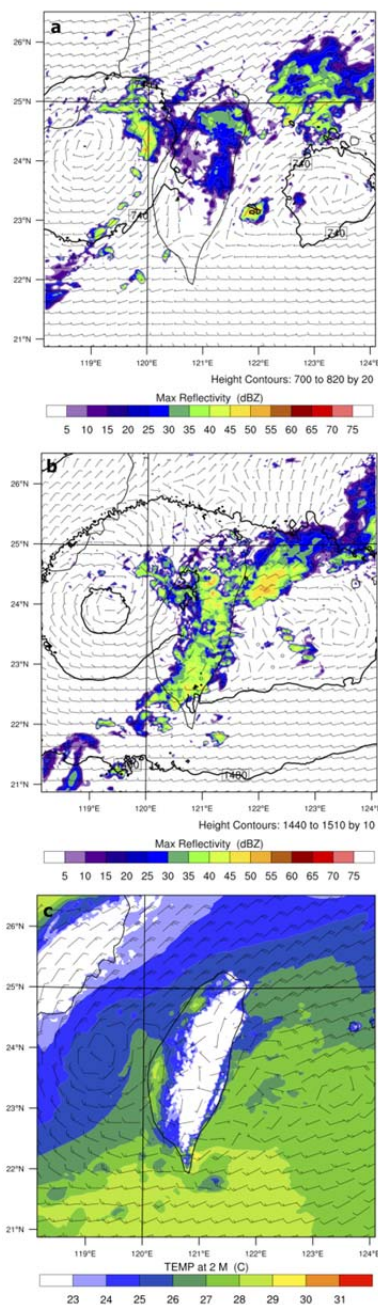


Fig. 5. WRF simulated (a) 925-hPa geopotential height (gpm, contoured), winds (1 barb= 10 m s^{-1}) and maximum reflectivity (dBZ, shaded) at 0000 UTC (0800 LT) and (b) 850-hPa geopotential height (gpm, contoured), winds (1 barb= 10 m s^{-1}) and maximum reflectivity (dBZ, shaded) at 0600 UTC (1400 LT) 31 May. (c) 10-m winds (1 full barb= 5 m s^{-1}) and 2-m temperature ($^{\circ}\text{C}$) at 0600 UTC (1400 LT) 31 May (model is initialized at 0000 UTC 30 May) (Domain 3, 3km resolution).

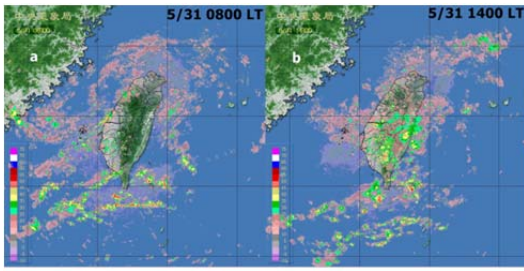


Fig. 6. (a) Mosaic radar reflectivities (dBZ) at 0800 LT (0000 UTC) and (b) 1400 LT (0600 UTC). (Courtesy of CWB).

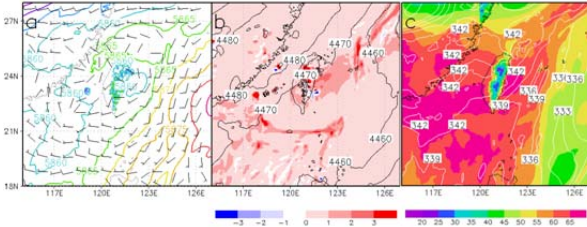


Fig. 7. WRF simulated (a) 500-hPa geopotential height (gpm) and winds (m s^{-1}), (b) 500-hPa absolute vorticity (10^{-4} s^{-1}) and 400-700-hPa thickness (gpm) and (c) total precipitable water (mm, shaded) and equivalent potential temperature (K, contoured) at 1800 UTC 15 June (0200 LT 16 June) (model is initialized at 1200 UTC 15 June) (Domain 2, 9km resolution).

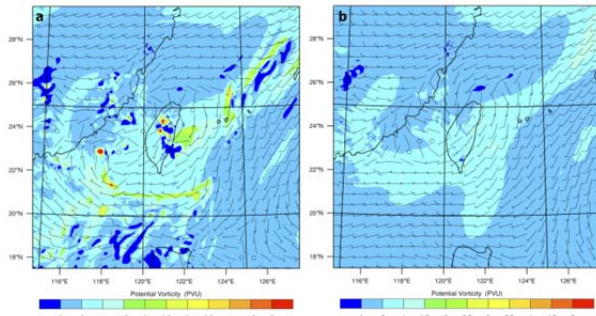


Fig. 8. WRF simulated (a) 500-hPa PV (PVU) and winds ($1 \text{ barb} = 10 \text{ m s}^{-1}$) in CTRL and (b) WOLH run at 1800 UTC 15 June (model is initialized at 1200 UTC 15 June) (Domain 2, 9km resolution).

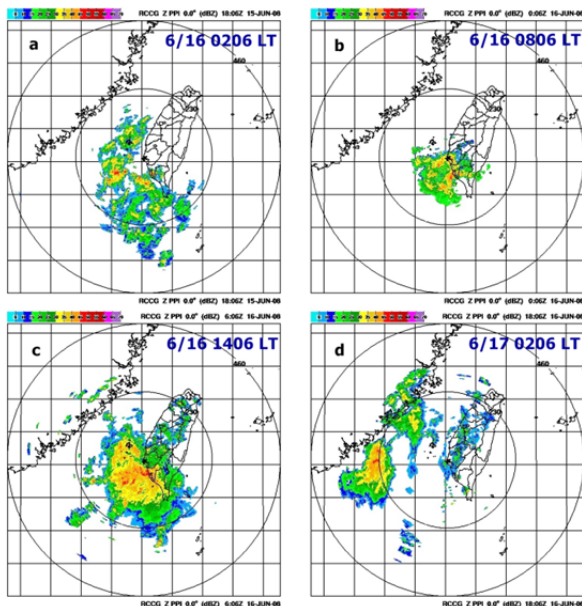


Fig. 9. Composite radar reflectivities (dBZ) at (a) 1806 UTC 15 June (0206 LT 16 June), (b) 0006 UTC (0806 LT) 16 June, (c) 0606 UTC (1406 LT) 16 June, and (d) 1806 UTC 16 June (0206 LT 17 June).

The local circulation also contributed to the development of the intense offshore convective line (Fig. 9a). On the early morning of 16 June (0200 LT) (15 June 1800 UTC), the broad southwesterly flow between the Mei-Yu trough over southeastern China and the

Western Pacific High east of Taiwan prevailed upstream of the southwestern Taiwan with a relative strong southwesterly wind axis east of Taiwan at low levels (Fig. 10a). The southwesterly flow with a relatively small westerly component was blocked and deflected by the CMR (Fig. 10a). With a weak westerly wind component and cold, dry katabatic flow over the windward southwestern slope of CMR (Fig. 10a), no rain showers developed over the southwestern slopes of Taiwan (Fig. 9a). The convergence between the decelerating southwesterly flow (orographic blocking) and land breezes/off shore flow (Figs. 10a and 10b) was evident and was favorable for the intensification of convective activity as they moved toward the island (Fig. 9a).

Time series of air temperature at three coastal stations (Station K, T and H in Figure 1c) showed the cool air over southwestern Taiwan due to rain evaporative cooling (Fig. 11) in agreement with Xu et al. (2012). Due to the combination of nocturnal and evaporative cooling over the southwestern coast region, orographic blocking was significant in the early morning. The results from this study are consistent with previous studies that nocturnal and evaporative cooling over the coastal region strengthens and deepens the cold katabatic/offshore flow on windward side of the island of Hawaii (Wang and Chen 1995; Carbone et al. 1998; Frye and Chen 2001; Feng and Chen 2001) and a recent modeling study over the southwestern Taiwan (C.-S. Chen et al. 2011).

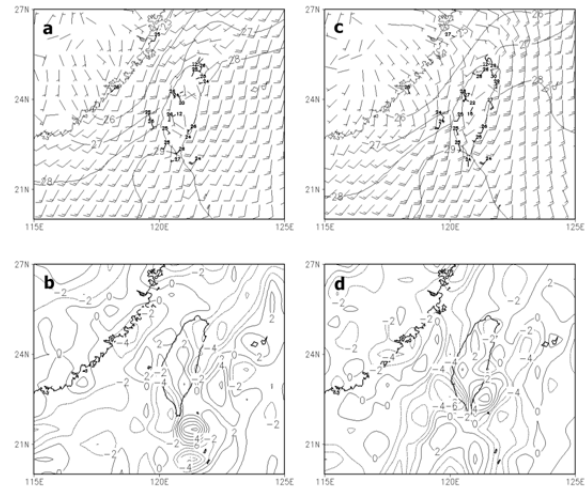


Fig. 10. (a) YOTC surface winds (Full barb represents 5 m s^{-1}) and sea surface temperature ($^{\circ}\text{C}$, contoured) and station surface winds (Full barb represents 5 m s^{-1}) and temperature ($^{\circ}\text{C}$) (thick), and (b) 1000-hPa divergence (10^{-5} s^{-1}) at 1800 UTC 15 June (0200 LT 16 June) 2008. (c) Surface winds (Full barb represents 5 m s^{-1}) and sea surface temperature ($^{\circ}\text{C}$, contoured) and station surface winds (Full barb represents 5 m s^{-1}) and temperature ($^{\circ}\text{C}$) (thick), and (d) 1000-hPa divergence (10^{-5} s^{-1}) at 0600 UTC (1400 LT) 16 June 2008.

At 1400 LT 16 June, the strong south-southwesterly axis (wind speed $> 10 \text{ m s}^{-1}$) shifted westward across the southwestern and southern Taiwan (Fig. 10c). The south-southwesterly winds were blocked and deflected by the southern part of the CMR with low-level winds paralleling the CMR downstream (Fig. 10c). The splitting of the southerly flow took place over the southern tip of Taiwan (Fig. 10c). Over the southwestern coast of Taiwan, the upstream southwesterly flow converged with the splitted southerly flow (Figs. 10c and 10d) resulting in favorable conditions for the intensification of convective activity (Fig. 9c). A similar scenario was recently simulated by C.S. Chen et al. (2010). With rain evaporation over southwestern Taiwan and relatively warm SST offshore (Fig. 10c), the daytime sea breezes-upslope flow was absent over the southwestern Taiwan (Fig. 10c). Therefore, no rainfall maximum over the mountain range due to absent of orographic lifting of airflow there.

c. Afternoon heavy rainfall associated with thunderstorm activity over northern Taiwan

Chen and Chan (1994) simulated the formation of orographic clouds and precipitation over leeside convergence zone (northern Taiwan) under a prevailing southerly monsoon flow during

a non-Mei-Yu case (20 June 1987). In their model, the moist airflow coming from the south was diverted near the southern tip of Taiwan, followed along the edges of CMR, and covered near the northern tip. The upward motion associated with the clouds and precipitation in the presence of afternoon surface heating could further help the development of this northern convergence.

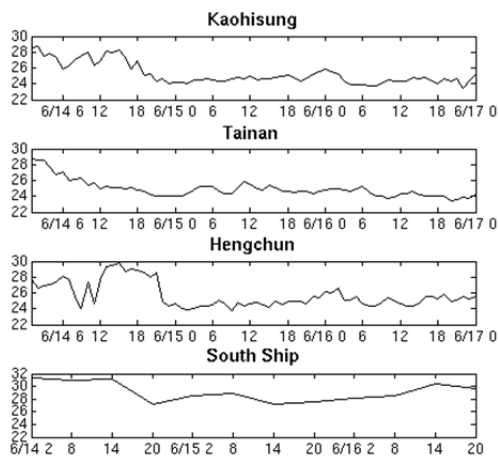


Fig. 11. Time series of surface temperature ($^{\circ}\text{C}$) during 14–16 June (LT) at 3 coastal stations, Kaohisung, Tainan and Hengchun (Station K, T and H in Figure 1c), and the air temperature ($^{\circ}\text{C}$) at the lowest level of shipboard soundings lunched every 6 h at South Ship.

In this Mei-Yu case, the northern tip of Taiwan in the afternoon hours of 16 June 2008 was also in the leeside wake zone/convergence zone with flow splitting over the southern tip of Taiwan (Fig. 10c), but the convergence was weak (Fig. 10d). With relatively weak convergence in the wake zone, relatively cold SSTs offshore, and afternoon solar heating, the pronounced sea breezes circulations and onshore/upslope flows were well developed over northern Taiwan (Fig. 10c), resulting in the development of cloud/rain systems and leading to heavy rainfall over this region (Fig. 9c).

5. Summary and Discussion

Two distinct heavy rainfall events during Mei-Yu season with rainfall maximum along the windward mountain range (31 May 2008 during TiMREX IOP#3) and the coast (16 June 2008 during IOP#8) over southwestern Taiwan were studied. For both cases, the existence of a moisture tongue rooted in the tropics provided moisture source for the pronounced latent heat release associated with the frontal rainband or the prefrontal MCSs, which led to PV generation and intensification of a Mei-Yu frontal mesocyclone at low levels (IOP#3) or an upper-level mesocyclone (IOP#8).

Two mesocyclones approaching Taiwan provided favorable large-scale conditions for the development of heavy rainfall over southwestern Taiwan. At 0000 UTC (0800 LT) 31 May (IOP#3), the strengthened southwesterly flow ahead of the Mei-Yu frontal mesocyclone approaching western Taiwan and blocked southerly flow along the CMR converged with the post-frontal northeasterly flow and land breezes which resulted in the formation of an intense coastal convective cell along the frontal boundary at central western coast of Taiwan. At 0600 UTC (1400 LT) 31 May, the development of the broad area convective system over the windward mountain slopes and mountain interior of central and southwestern Taiwan after the passage of surface front was contributed by orographic lifting of (1) the pre-existing convective cell along the frontal boundary that propagated inland and (2) strengthened warm, moist southwesterly flow ahead of the mesocyclone combined with sea breezes-upslope flow on the windward slopes during the passage of the upper-level short-wave trough.

At 1800 UTC 15 June (0200 LT 16 June) (IOP#8), a 500-hPa vorticity maximum was associated with the upper-level mesocyclone over Taiwan. Pronounced southeastward vorticity advection by thermal wind contributed to the development of convection off the southwest coast of Taiwan. In addition, the local circulation also played a role in triggering the offshore convective

line. The convergence between the decelerating southwesterly flow (orographic blocking enhanced by nocturnal and rain evaporative cooling) and land breezes/off shore flow was evident and was favorable for the intensification of convective activity as they moved toward the island. During the day, the rain evaporative cooling associated with MCSs over the coastal region of southwestern Taiwan induced significant blocking of southwesterly flow and turning of southwesterly flow to southerly mountain-parallel flow over the blocked region. Due to the warm SST underneath, the air temperature near the surface over the ocean off the southwestern coast was warmer than over coastal land. As a result, sea breezes were not possible to develop. In addition, the orographic lifting of the moist monsoon flow over the southwestern windward slopes of CMR was absent due to the prevailing of the mountain-parallel flow aloft. Thus, no rainfall maximum developed in the mountain interior on 16 June. Over northern Taiwan, with relatively weak convergence in the wake zone, relatively cold SSTs offshore, and afternoon solar heating over land, the pronounced sea breezes circulations and onshore/upslope flows were well developed over northern Taiwan, resulting in heavy rainfall associated with thunderstorm activity during IOP#8.

References

- Carbone, R. E., J. D. Tuttle, W. A. Cooper, V. Grubisic, and W.-C. Lee, 1998: "Trade wind rainfall near the windward coast of Hawaii", *Mon. Wea. Rev.*, 126, 2847–2863.
- Chen, C.-S., and Y.-O. E. Chan, 1994: "On the formation of cloud and precipitation systems in Taiwan during TAMEX IOP #11", *Terr. Atmos. Oceanic Sci.*, 5, 137–168.
- _____, W.-C. Chen, Y.-L. Chen, P.-L. Lin, and S.-J. Lai, 2005: "An investigation of orographic effects on two heavy rainfall events over southwestern Taiwan during the Mei-Yu season", *Atmos. Res.*, 73/1-2, 101–130.
- _____, Y.-L. Chen, P.-C. Lin, P.-L. Lin, C.-L. Liu, C.-J. Su, and W.-C. Peng, 2008: "An investigation of extremely heavy rainfall events over southwestern Taiwan during the Mei-Yu season from 1997–2006", *Atmos. Sci.*, 35, 287–304 (In Mandarin with English Abstract). (Available from Meteor. Soc. of the Rep. of China, 64 Kung-Yuan Road, Taipei, Taiwan)
- _____, C.-L. Liu, P.-L. Lin, and W.-C. Chen, 2007: "Statistics of heavy rainfall occurrences in Taiwan", *Wea. Forecasting*, 22, 981–1002.
- _____, Y.-L. Lin, W.-C. Peng, and C.-L. Liu, 2010: "Investigation of a heavy rainfall event over southwestern Taiwan associated with a subsynoptic cyclone during the 2003 Mei-Yu season", *Atmos. Res.*, 95, 235–254.
- _____, N.-N. Hsu, C.-L. Liu, and C.-Y. Chen, 2011: "Orographic effects on localized heavy rainfall events over southwestern Taiwan on 27 and 28 June 2008 during the post-Mei-Yu period", *Atmos. Res.*, 101, 595–610.
- Chen, F., and J. Dudhia, 2001: "Coupling an advanced land surface–hydrology model with the Penn State–NCAR MM5 modeling system. Part I: Model implementation and sensitivity", *Mon. Wea. Rev.*, 129, 569–585.
- Chen, Y.-L., and J. Li, 1995: "Characteristic of surface airflow and pressure patterns over the island of Taiwan during TAMEX", *Mon. Wea. Rev.*, 123, 695–716.
- Davis, C. A., and W.-C. Lee, 2012: "Mesoscale analysis of heavy rainfall episodes from SoWMEX/TiMREX", *J. Atmos. Sci.*, 69, 521–537.
- Dudhia, J., 1989: "Numerical study of convection observed during the winter monsoon experiment using a mesoscale two-dimensional model," *J. Atmos. Sci.*, 46, 3077–3107.
- Feng, J., and Y.-L. Chen, 2001: "Numerical simulations of airflow and cloud distributions over the windward side of the island of Hawaii. Part II: Nocturnal flow regime", *Mon. Wea. Rev.*, 129, 1135–1147.
- Ferrier, B. S., Y. Jin, Y. Lin, T. Black, E. Rogers, and G. DiMego, 2002: "Implementation of a new grid-scale cloud and precipitation scheme in the NCEP Eta Model", 19th Conf. on Weather Analysis and Forecasting/15th Conf. on Numerical Weather Prediction, San Antonio, TX, Amer. Meteor. Soc., 280–283.
- Frye, J., and Y.-L. Chen, 2001: "Evolution of downslope flow under strong opposing trade winds and frequent trade-wind rain showers over the island of Hawaii", *Mon. Wea. Rev.*, 129, 956–977.

- Gemmill, W., B. Katz, and X. Li, 2007: "Daily real-time global sea surface temperature-high resolution analysis", NOAA/NCEP, NOAA/NWS/NCEP/MMAB Office Note Nr. 260, 39 pp.
- Hong, S.-Y., Y. Noh, and J. Dudhia, 2006: "A new vertical diffusion package with an explicit treatment of entrainment processes", *Mon. Wea. Rev.*, 134, 2318-2341.
- Janjic, Z. I., 1994: "The step-mountain eta coordinate model: further developments of the convection, viscous sublayer and turbulence closure schemes", *Mon. Wea. Rev.*, 122, 927-945.
- _____, 2000: "Comments on "Development and Evaluation of a Convection Scheme for Use in Climate Models"", *J. Atmos. Sci.*, 57, p. 3686.
- Johnson, R. H., and J. F. Bresch, 1991: "Diagnosed characteristics of precipitation systems over Taiwan during the May-June 1987 TAMEX", *Mon. Wea. Rev.*, 119, 2540-2557.
- Kerns, B., Y.-L. Chen, and M.-Y. Chang, 2010: "The diurnal cycle of winds, rain and clouds over Taiwan during the Mei-Yu, Summer, and Autumn regimes", *Mon. Wea. Rev.* 138, 497-516.
- Kuo, Y.-H., and G. T.-J. Chen, 1990: "The Taiwan area mesoscale experiments: An overview", *Bull. Amer. Meteor. Soc.*, 71, 488-503.
- Li, J., and Y.-L. Chen, 1998: "Barrier jets during TAMEX", *Mon. Wea. Rev.*, 126, 959-971.
- _____, _____, and W.-C. Lee, 1997: "Analysis of a heavy rainfall event during TAMEX", *Mon. Wea. Rev.*, 125, 1060-1082.
- Mlawer, E. J., S. J. Taubman, P. D. Brown, M. J. Iacono, and S. A. Clough, 1997: "Radiative transfer for inhomogeneous atmosphere: RRTM, a validated correlated-k model for the longwave", *J. Geophys. Res.*, 102 (D14), 16663-16682.
- Rogers, E., T. Black, B. Ferrier, Y. Lin, D. Parrish, and G. DiMego, 2001: "Changes to the NCEP Meso Eta Analysis and Forecast System: Increase in resolution, new cloud microphysics, modified precipitation assimilation, modified 3DVAR analysis", NWS Technical Procedures Bulletin 488, NOAA/NWS, 2001. [Available at <http://www.emc.ncep.noaa.gov/mmb/mmbpl/eta12tpb/>]
- Skamarock, W. C., J. B. Klemp, J. Dudhia, D. O. Gill, D. M. Barker, M. G. Duda, X.-Y. Huang, W. Wang, and J. G. Powers, 2008: "A description of the Advanced Research WRF Version 3", NCAR Tech Notes-475+STR, 113 pp.
- Wang, J.-J., and Y.-L. Chen, 1995: "Characteristics of near-surface wind and thermal profiles on the windward slopes of the island of Hawaii", *Mon. Wea. Rev.*, 123, 3481-3501.
- Waliser, D.E., and Coauthors, 2012: "The "Year" of Tropical Convection (May 2008 to April 2010): Climate Variability and Weather Highlights", *Bull. Amer. Meteorol. Soc.*, in press.
- Xu, W., E. J. Zipser, Y.-L. Chen, C. Liu, Y.-C. Liou, W.-C. Lee, and B. J.-D. Jou, 2012: "An orography-associated extreme rainfall event during TiMREX: initiation, storm evolution, and maintenance", *Mon. Wea. Rev.*, in press.
- Yeh, H.-C., and Y.-L. Chen, 1998: "Characteristics of the rainfall distribution over Taiwan during TAMEX," *J. Appl. Meteor.*, 37, 1457-1469.